Available online at www.sciencedirect.com

ScienceDirect

Proceedings of the Combustion Institute 35 (2015) 1501–1508

Proceedings of the Combustion Institute

www.elsevier.com/locate/proci

Propagation speeds of expanding turbulent flames of C_4 to C_8 *n*-alkanes at elevated pressures: Experimental determination, fuel similarity, and stretch-affected local extinction

Fujia Wu [a,*], Abhishek Saha [a], Swetaprovo Chaudhuri [a], Chung K. Law [a,b]

[a] *Department of Mechanical and Aerospace Engineering Princeton University, Princeton, NJ 08544, USA*
[b] *Center for Combustion Energy Tsinghua University, Beijing 100084, China*

Available online 22 August 2014

Abstract

In this study we experimentally investigated the propagation and the associated propagation speeds of expanding C_4 to C_8 *n*-alkane flames in near-isotropic turbulence, from 1 to 5 atm, using a *constant-pressure*, dual-chamber, fan-stirred vessel. The motivation of the work is to explore whether the previously observed fuel similarity for C_4–C_8 *n*-alkanes for laminar flames also holds for turbulent flames, and to investigate the possible influence of mixture nonequidiffusion on the stretch-affected flame structure especially the occurrence of local extinction. Extensive results show that within the present parametric range of investigation, relevant for the flamelet and thin-reaction zones in the conventional turbulent combustion regime diagram, the turbulent flame speeds of stoichiometric and rich mixtures of these fuels, whose Lewis numbers (*Le*) are close to or smaller than unity, indeed assume similar values at various pressures, equivalence ratios and turbulence intensities. However, the corresponding lean flames, whose *Le* is greater than unity, exhibit strong propensity of local extinction, ostensibly caused by local stretch through the $Le > 1$ mixture nonequidiffusion.

Keywords: Turbulent flame; Spherical flame; Flame speed scaling; Fuel similarity; *n*-Alkanes

1. Introduction

Combustion chemistry of large practical fuels involves hundreds to thousands of compounds and even larger numbers of reactions [1], which are difficult to track at the fundamental level. A simplified approach is based on the assumption that large fuels crack rapidly as compared to the subsequent oxidation of cracked intermediates [2,3]. As a result, it is the oxidation of the cracked products that determines the rates of radical pool build-up and heat release. Consequently a detailed description of the cracking process may not be necessary as long as the major cracked product

* Corresponding author. Address: D103 Engineering Quad, MAE, 59 Olden Street, Princeton University, NJ 08544, USA. Fax: +1 (609) 258 6233.
E-mail address: fujiawu@princeton.edu (F. Wu).

http://dx.doi.org/10.1016/j.proci.2014.07.070
1540-7489/

distribution is well predicted. Such a concept has been explored for the global parameters of laminar flames [4–6], particularly for *n*-alkanes [3–5, 7–11], demonstrating that the associated laminar flame speeds [4,5,9], its sensitivity to stretch through the Markstein length [5], laminar premixed flame and extinction strain rates [4] largely assume similar values. This supports the use of similarity rules for rates of fuel-related reactions [10]. In view of the usefulness of this concept, it therefore behooves us to extend the investigation to the more complex and practically prevalent system of turbulent flames, recognizing the possible intrusion of turbulent eddies into the flame structure, with effects that are as yet not clearly understood.

In addition to the issue of fuel similarity, we further note that while there are a large number of measurements for the laminar flame speeds of large *n*-alkanes, well-defined measurements of turbulent flame speeds are rather scarce. Availability of such data would facilitate the study of turbulence-chemistry interactions [12] because of the moderately well-established kinetic mechanisms of the *n*-alkanes, as well as the development and validation of turbulent combustion models such as that of Large Eddy Simulation (LES).

In the present study, the turbulent flame speeds of C_4–C_8 *n*-alkanes were experimentally measured for expanding turbulent flames over a wide range of turbulence intensities and equivalence ratios, in the pressure range of 1–5 atm. The results provide useful data for further studies of the structure and modeling of turbulent flames, allow direct and consistent assessment of fuel similarity for *n*-alkanes under different flow and flame conditions, and yield useful observation on the occurrence of stretch-affected local extinction. It should be noted that the goal of this work is not to seek a unified scaling for turbulent flame speeds for all conditions, which remains to be an open question, but rather to investigate the applicability fuel similarity for *n*-alkanes. However, the data presented here will be useful for future effort to arrive at a scaling relation for turbulent flame speeds.

2. Experimental setup

The experiments were conducted in a dual-chamber, fan-stirred, nearly constant-pressure vessel. It has been used for measuring both laminar [5,6,13] and turbulent flame speeds [14,15]; detailed description of the experimentation and data analysis are given in the cited references. The vessel incorporates a dual-chamber pressure release mechanism to allow flame propagation in near-constant pressure. The operating conditions are identical to those reported in [14,15], except that the vessel is now heated up to 353 K by covering the outer chamber with multiple silicon electrical heaters for experimentation with liquid fuels. Turbulence is generated by four orthogonally positioned fans which continuously run during the entire flame propagation event. The fan-generated, non-reacting turbulent flow field was characterized by high-speed particle image velocimetry (HS-PIV). Detailed flow-field statistics and quantification of the small but unavoidable deviation from isotropy are given in [14]. Turbulent flame speed measured by direct high-speed Schlieren imaging.

3. Results

3.1. Laminar flame speeds of C_4–C_8 n-alkanes

It has been shown in [5] that laminar flame speeds, S_L, for C_4–C_8 *n*-alkanes flames are similar at the initial temperature 353 K and pressures from 1 to 20 atm. In [9] it was also shown that C_4–C_8 *n*-alkanes assumes similar flame speeds at 1 atm and initial temperature 298 K. To establish the laminar flame speeds for current experiments at 353 K and to complement the flame speed data of C_4–C_8 *n*-alkanes at elevated temperatures reported in [5], we conducted additional measurements on *n*-butane/air mixtures at 353 K for 1–5 atm. The results, plotted in Fig. 1, show that *n*-butane indeed has similar flame speeds as the *n*-alkanes with longer carbon chain.

3.2. Regimes of turbulent flame conditions

The present study reports data for four fuels: *n*-butane, *n*-pentane, *n*-hexane and *n*-octane at three different pressures, 1, 2 and 5 atm. The laminar flames in this pressure range do not exhibit

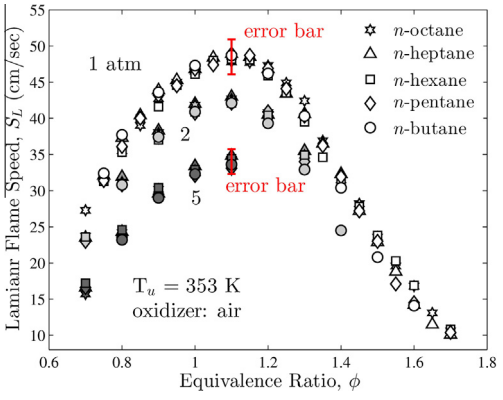

Fig. 1. Measured laminar flame speeds for C_4–C_8 *n*-alkanes. C_5–C_8 data are taken from [5]. The error bar for S_L at these conditions is ±5% according to recent direct numerical simulations of expanding spherical flames [24].

intrinsic flamefront instabilities; therefore the interaction between turbulence and flamefront instabilities is removed. Table 1 summarized the mixture and flame properties of the conditions considered in this study, with *n*-hexane being an example. Due to fuel similarity, the values are similar for other fuels except for *Le*, which is separately listed in Table 2. In addition to the stoichiometric condition at $\phi = 1.0$, lean mixtures at $\phi = 0.8$ and rich mixtures at $\phi = 1.4$ are selected because these flames have similar laminar flame speed S_L and laminar flame thickness δ_L; therefore the effect of differential diffusion can be independently studied.

The differential diffusion properties of a combustible premixture are characterized by the Lewis number *Le* and Markstein number Mk_L [16]. The Lewis number Le_i of any species i is defined as $Le_i = \alpha/D_i$, where α is an average thermal diffusivity of the mixture and D_i is a mixture-averaged mass diffusivity of species i with respect to the mixture [16]. In Tables 1 and 2, at $\phi = 0.8$ *Le* is defined as Le_{Fuel} at $\phi = 1.4$, Le_{O2} at $\phi = 1.0$ and 0.5 ($Le_{\text{Fuel}} + Le_{O2}$). Mk_L is defined as $\delta_{M,b}/\delta_L$, where $\delta_{M,b}$ is the Markstein length with respect to the burned gas [5]. It is seen from Table 1 that at $\phi = 0.8$ and 1.0, we have $Le > 1$ and $Mk_L > 0$, and at $\phi = 1.4$, we have $Le < 1$ and $Mk_L < 0$.

We experimented with fan speeds from 2000 to 7500 rpm, which results in cold flow turbulence intensity, u_{rms}, varying from 1.4 to 5.4 m/s. The longitudinal integral scale, L_I, was calculated to be 0.4 cm, from the cold flow statistics by integrating the two-point velocity correlation function. The turbulent Reynolds number, $Re_T = u_{\text{rms}} L_I/v$ (where v is the kinematic viscosity) based on the cold flow properties varies from 400 to 7400, and the Taylor Reynolds number, $Re_T = u_{\text{rms}}\lambda_g/v$ varies from 51 to 221, using the relation $Re_\lambda = (20Re_T/3)^{1/2}$ [17], where λ_g is the Taylor microscale. Figure 2 plots the conditions of the present experiments in the Borghi diagram. It is seen that most experiments fall in the so-called corrugated flamelet and thickened flamelet regimes.

3.3. Interpretation of expanding flame propagation

From the Schlieren images, the area A enclosed by the flame edge can be calculated through edge detection method, while the mean flame radius is defined as $\langle R\rangle = \sqrt{A/\pi}$. By differentiating the $\langle R\rangle$ history with respect to time, the flame propagation speed $d\langle R\rangle/dt$ can be determined. The simultaneous measurements using Schlieren imaging and Mie scattering in [18] suggest that $d\langle R\rangle/dt$ corresponds to the turbulent displacement speed for the progress variable $c = 0.05$–0.1.

Before presenting the results of different fuels, it is necessary to demonstrate how we interpret and scale turbulent flame speeds measured from expanding flames. If the flame structure is assumed to be unaffected, the problem of turbulent flame propagation can be considered as a geometric process in which the effect of turbulence is to wrinkle the flame at a multitude of length scales. Such a problem was considered in [19] for statistically planar flames based on the spectrum closure of an iso-surface for flamefront by Peters [20]. It was shown that for mixtures with fixed

Table 1
Laminar flame properties of *n*-hexane/air. S_L and Markstein number Mk_b are from experiments using the present vessel [5], except the condition $\phi = 1.0$ and 1.4 at 2 and 5 atm, at which S_L and Mk_b cannot be measured due to flamefront instability. S_L at $\phi = 1.0$ and 1.4 at 2 and 5 atm, and T_{ad} and δ_L are calculated by Chemkin II EQUIL, TRANSPORT and PREMIX packages using JetSurF 2.0 chemistry model [3]. The unburned gas temperature T_u is 353 K in all cases.

P, atm	ϕ	T_{ad}, K	S_L, cm/s	δ_L, cm	Mk_L	Θ
1	0.8	2115	35.6	0.044	2.55	6.27
1	1.0	2312	48.2	0.037	2.27	6.99
1	1.4	2080	33.3	0.046	−0.83	6.85
2	0.8	2119	30.2	0.025	2.76	6.27
2	1.0	2332	41.2	0.021	2.29	7.0
2	1.4	2078	25.4	0.029	N/A	6.86
5	0.8	2122	24.6	0.012	3.17	6.28
5	1.0	2356	32.7	0.010	1.80	7.1
5	1.4	2080	15.9	0.017	N/A	6.86

Table 2
Le of fuel/air mixtures by the Chemkin II TRANSPORT package using the transport properties in the JetSurF 2.0 chemistry model. *Le* does not change with pressure for idea gas.

ϕ	*n*-butane	*n*-pentane	*n*-hexane	*n*-octane
0.8	1.7	1.9	2.0	2.3
1.0	1.4	1.5	1.6	1.8
1.4	0.9	0.9	0.9	0.9

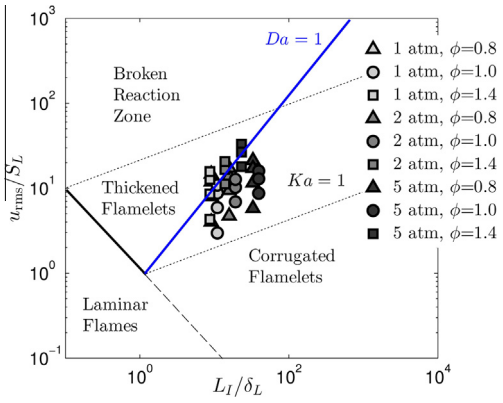

Fig. 2. Regimes of the present experimental conditions on Borghi diagram. S_L and δ_L of only *n*-hexane/air are used since other C_4–C_8 *n*-alkanes have almost the same values.

Le or Mk_L the normalized turbulent flame speed scales with the following expression,

$$\frac{S_T}{S_L} \propto \sqrt{\frac{u_{rms} L_I}{S_L \delta_L}} \tag{1}$$

A special property of turbulent expanding flames is that their speeds always increase as they expands, and so far there is no evidence that an equilibrium speed has been reached. In Fig. 3a, we plot the raw data $\langle R \rangle$ versus time for *n*-hexane/air flames at $\phi = 1.0$. It is seen all flames at different u_{rms} and pressure concave upward, indicating flame acceleration. It is seen that this acceleration mechanism is not contained in Eq. (1). Bradley et al. [21] attributed the acceleration to the effect of wrinkling of flame surface by vortices of increasing size during flame expansion. In view of this consideration, we consider a quantity that represents the effective turbulence intensity an expanding flame experiences,

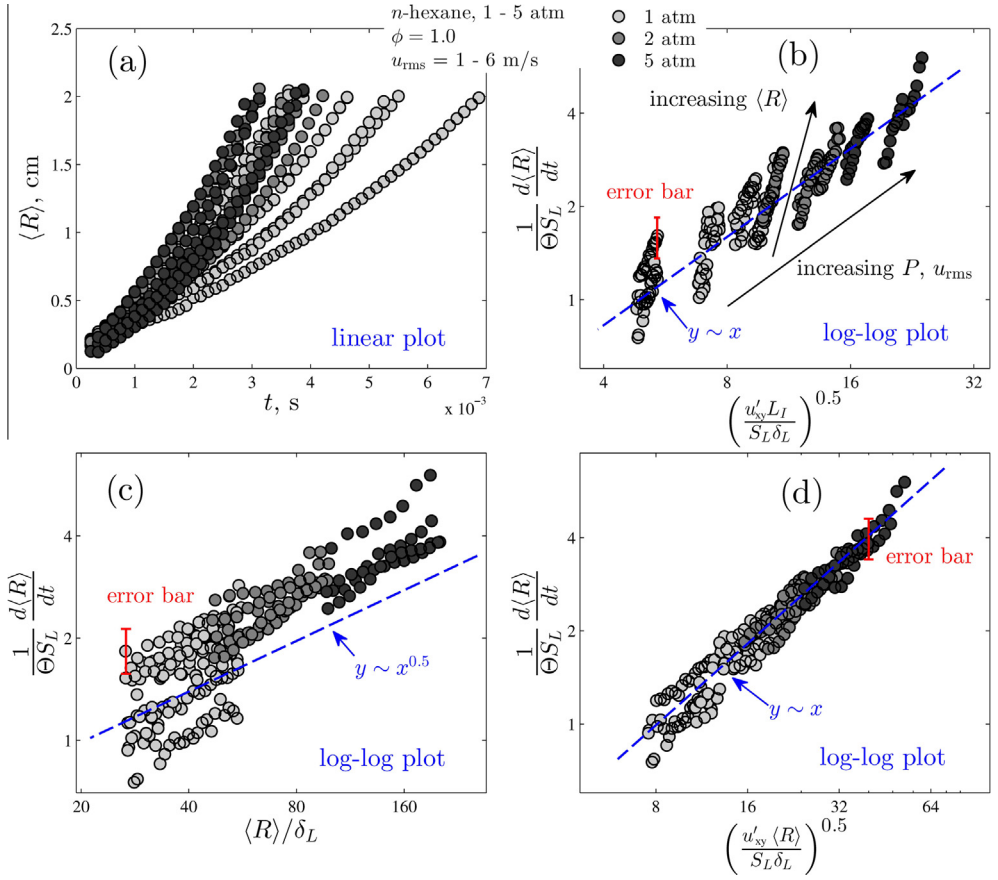

Fig. 3. (a) Raw experimental flame propagation data for *n*-hexane at $\phi = 1.0$. (b) Normalized $d\langle R \rangle/dt$ plotted with the scaling based on u'_{xy}. (c) Normalized $d\langle R \rangle/dt$ plotted with $\langle R \rangle/\delta_L$, (d) normalized $d\langle R \rangle/dt$ plotted with $Re_{T,f}^{1/2}$. The error bar represents ±15% random uncertainty in $d\langle R \rangle/dt$, which is calculated based on the 95% confidence interval of seven repeated runs on stoichiometric CH_4/air flame for a fixed experimental condition conducted in [15] (see the supplementary material).

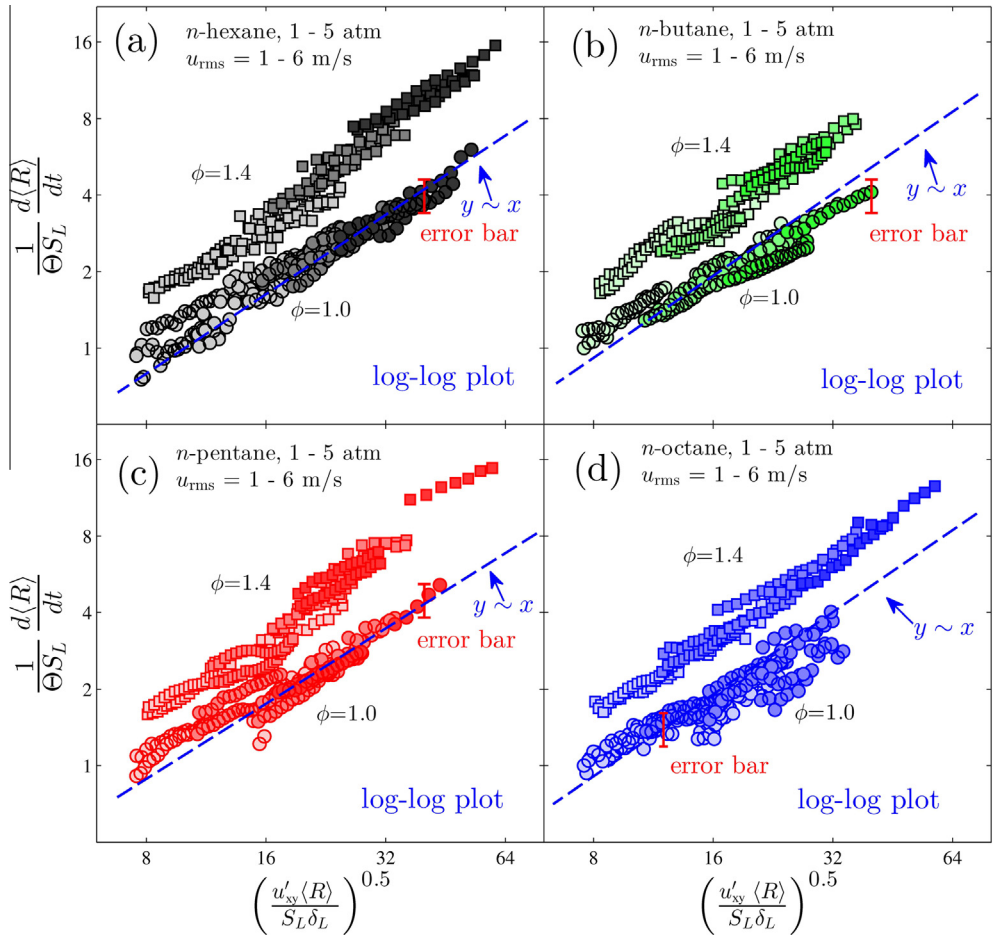

Fig. 4. Normalized $d\langle R\rangle/dt$ for (a) *n*-hexane, (b) *n*-butane, (c) *n*-pentane and (d) *n*-octane plotted with $Re_{T,f}^{1/2}$, for $\phi = 1.0$ and 1.4. The error bar represents ±15% random uncertainty in $d\langle R\rangle/dt$, see caption of Fig. 3.

$$u'_{xy} = \overline{\left[\frac{1}{2}\left(\left\langle (u_x - \langle u_x\rangle_R)^2\right\rangle_R + \left\langle (u_y - \langle u_y\rangle_R)^2\right\rangle_R\right)\right]^{0.5}} \quad (2)$$

where bar $\overline{(\cdot)}$ denotes time average, $\langle\cdot\rangle_R$ indicates spatial average over a 1 mm circular strip around radius R centering at the center of the chamber, and u_x and u_y are the measured instantaneous velocity from 2D HS-PIV. It is found from recent measurements [22] that u'_{xy} correlates with the fan speed rpm and $\langle R\rangle$ via $u'_{xy} = 0.002339 \times \text{rpm} \times \langle R\rangle^{0.33}$, where the units of u'_{xy} and $\langle R\rangle$ are m/s and m, respectively. Figure 3b plots the normalized $d\langle R\rangle/dt$ against $\sqrt{u'_{xy}L_I/S_L\delta_L}$, *i.e.*, Eq. (1) after replacing u_{rms} by u'_{xy}, for the data of *n*-hexane/air at $\phi = 1.0$ (with fixed Mk_L). It is however observed that only increase in u'_{xy} cannot adequately explain strong flame acceleration. While the data at different pressures follow the scaling quite well (for a fixed flame size), which comes from the contributions of S_L and δ_L, the data of individual runs, *i.e.* at various flame radius, do not follow this scaling, indicating there is stronger dependence on $\langle R\rangle$ than that is not captured in u'_{xy}. Figure 3c plots the normalized flame speed against $\langle R\rangle/\delta_L$. It is seen that all the data approximately follow a $\langle R\rangle^{1/2}$ dependence, while u'_{xy} only gives a $\sqrt{\langle R\rangle^{0.33}} \sim \langle R\rangle^{0.16}$ dependence through Eq. (1). Re-visiting the analysis in [19,20], we note that the flame brush thickness, δ_T, is assumed to be proportional to L_I. However, our recent measurement on δ_T using Mie scattering [15] showed that it increases with the flame size and is approximately proportional to $\langle R\rangle$. Therefore it is reasonable to seek the following scaling,

$$\frac{S_T}{S_L} \propto \sqrt{\frac{u'_{xy}\langle R\rangle}{S_L\delta_L}} \equiv Re_{T,f}^{1/2} \quad (3)$$

where L_I is replaced by $\langle R\rangle$. Figure 3d plots the scaling of Eq. (3) for *n*-hexane/air data at ϕ

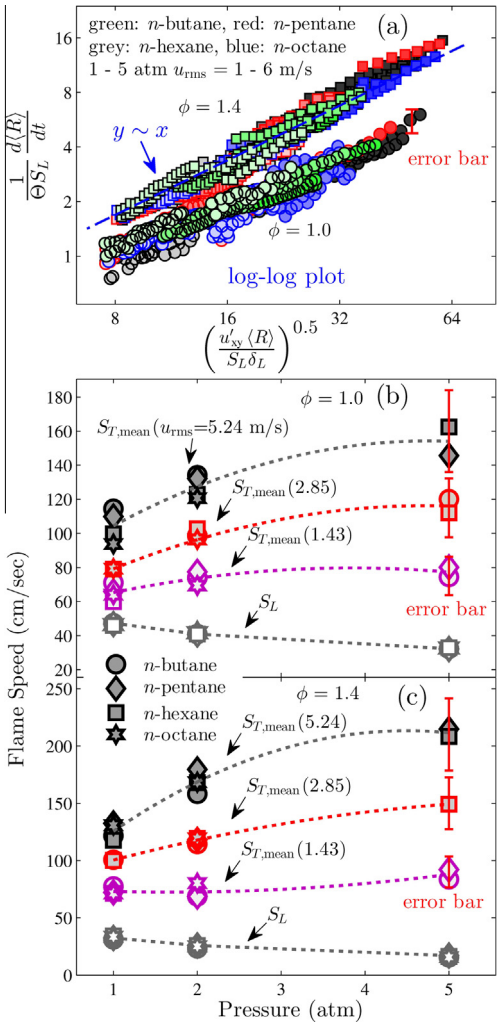

Fig. 5. (a) Normalized $d\langle R\rangle/dt$ versus $Re_{T,f}^{0.5}$ for *n*-pentane, *n*-hexane and *n*-octane mixtures for $\phi = 1.0$ and 1.4. (b and c) $S_{T,mean}$ for each individual run as a function of pressure and u_{rms} at $\phi = 1.0$ and $\phi = 1.4$. The error bar represents ±15% random uncertainty in $d\langle R\rangle/dt$, see caption of Fig. 3.

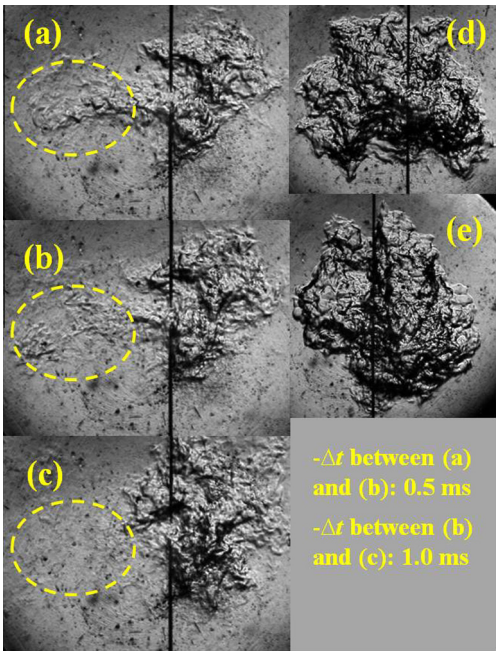

Fig. 6. Schlieren images of *n*-octane/air flames at 1 atm with $u_{rms} = 5.24$ m/s for (a–c) $\phi = 0.8$, (d) $\phi = 1.0$, (e) $\phi = 1.4$ showing the large area of local extinction for $\phi = 0.8$, while other conditions do not show such events.

= 1.0, and it is seen that now all the data collapse approximately onto one line, including both the pressure dependence and slopes of individual-run data. Such a scaling was also previously demonstrated for H_2, C_1–C_4 hydrocarbons and DME for a wide range of conditions [14,15]. In the present study, Eq. (3) is used to present our results and discuss fuel similarity.

3.4. Fuel similarity in C_4–C_8 *n*-alkanes

Figure 4 shows the normalized turbulent flame speeds versus $Re_{T,f}^{1/2}$ for $\phi = 1.0$ and 1.4 for *n*-butane, *n*-pentane, *n*-hexane and *n*-octane, respectively. To eliminate the influence of effects of ignition and chamber wall, only data in the range of 1.0 cm $< \langle R\rangle <$ 2.0 cm were considered and plotted. From Fig. 4a, it is seen that all the data at $\phi = 1.4$ also follow the $Re_{T,f}^{1/2}$ scaling well, but it has a much higher prefactor, resulting uniformly higher normalized turbulent flame speed than the data at $\phi = 1.0$ in the log–log plots. From Fig. 4b–d, it is also observed that for the other three fuels, turbulent flame propagation approximately follows $Re_{T,f}^{1/2}$ scaling for each individual mixture, and the prefactor for data at $\phi = 1.4$ is always higher than that of $\phi = 1.0$. The higher normalized turbulent flame speeds at $\phi = 1.4$ compared to $\phi = 1.0$ is due to the thermodiffusive effects, *i.e.*, the lower values of *Le* and Mk_L. A unified scaling law for turbulent flame speeds that includes the thermodiffusive effects is a recognized challenge [23]. An attempt was made in [15] for flames with $Mk_L > 0$. However, since $Mk_L < 0$ for all the conditions at $\phi = 1.4$, it is not possible to collapse the data at different ϕ using the scaling proposed in [15]. Nevertheless, data in Fig. 4 suggest the general applicability of Eq. (3) for mixtures with fixed Mk_L (ϕ or *Le*).

To test the concept of fuel similarity, Fig. 5a shows all the data for *n*-butane, *n*-pentane, *n*-hexane and *n*-octane in terms of $Re_{T,f}^{1/2}$ scaling in one plot. It is seen that the data for different fuels collapse reasonably well for both small and large

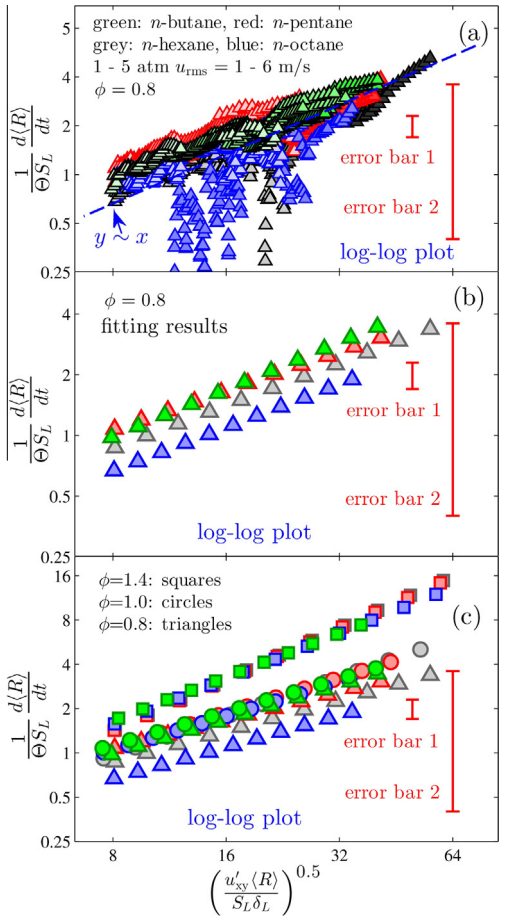

Fig. 7. (a) Normalized $d\langle R\rangle/dt$ for *n*-hexane, *n*-butane, *n*-pentane and *n*-octane plotted with $Re_{T,f}^{1/2}$ for $\phi = 0.8$; (b) Linearly fitted results of normalized $d\langle R\rangle/dt$ against $Re_{T,f}^{1/2}$ for each fuel at $\phi = 0.8$; (c) Linearly fitted results of normalized $d\langle R\rangle/dt$ against $Re_{T,f}^{1/2}$ for all fuels and ϕ. Since the flame may or may not exhibit local extinctions, two error bars are plotted for (a). Error bar 1 in (a) represents ±15% random uncertainty in $d\langle R\rangle/dt$, see caption of Fig. 3. Error bar 2 in (a) represents ± 80% random uncertainty obtained from the 95% confidence interval from the four repeated experiments on *n*-hexane at $\phi = 0.8$ (see the supplementary material). Error bars in (b) represent 95% confidence interval of the linear fittings of normalized $d\langle R\rangle/dt$ against $Re_{T,f}^{1/2}$.

values of $Re_{T,f}$. Consequently, the validity of fuel similarity for C_4–C_8 *n*-alkanes is strongly suggested for such conditions, *i.e.*, stoichiometric and rich flames with air from 1 to 5 atm in corrugated and thickened flame regimes. In addition, Fig. 5b–c also plots the averaged propagation speed, $S_{T,\mathrm{mean}}$, defined as

$$S_{T,\mathrm{mean}} = \frac{3\int_{\langle R\rangle_1}^{\langle R\rangle_2}\langle R\rangle^2(d\langle R\rangle/dt)d\langle R\rangle}{\Theta(\langle R\rangle_2^3 - \langle R\rangle_1^3)} \quad (4)$$

where Θ is the thermal expansion ratio, and $\langle R\rangle_1$ and $\langle R\rangle_2$ are 1.0 and 2.0 cm, respectively. It is seen that while laminar flame speeds decrease with pressure, $S_{T,\mathrm{mean}}$ increase with pressure, and all the C_4–C_8 *n*-alkanes have similar values for both.

3.5. Stretch-induced local extinction

We have also conducted experiments at $\phi = 0.8$ for a wide range of turbulence intensities and pressures. First, we examine the difference in the flame morphology between fuel-lean and stoichiometric and fuel-rich flames, as illustrated in Fig. 6 for typical images of *n*-octane flames. It is clearly seen that while the flame images at $\phi = 1.0$ and 1.4 show clear contours of the flamefront, those at $\phi = 0.8$ on the contrary show that the flamefront locations cannot be sharply identified in extensive regions of the flame ensemble and the burning seems to spread out into multiple, loosely-connected, regions. For $\phi = 0.8$, we also observed local extinction as the flame propagates. Fig. 6(a–c) shows a series of flame images for *n*-octane, where local extinction can be clearly identified at the marked zones. The occurrence of local extinction (as versus global extinction) over such a large region also suggests possible re-ignition since extinction leads to unburned hot fuel/air pockets which could re-ignite at another instant and location. Thus in spite of the fact that the conditions for $\phi = 0.8$ fall at almost the same location as those for $\phi = 1.0$ and 1.4 in the regime diagram, the nature of burning turns out to be quite distinct for these two cases. This observation implies that effects of non-equidiffusion need to be incorporated in a more generalized construction of the regime diagram to capture all possible effects.

We further note that local extinction and the blurry flame edge pose significant challenge in tracking or even defining the "flamefront" location. Nevertheless, we still conducted the tracking using the canny edge detection algorithm in Matlab. In addition, multiple runs were repeated at the same condition to obtain more data for averaging. Fig. 7(a) plots the normalized turbulent flame speed versus $Re_{T,f}^{1/2}$ at $\phi = 0.8$ for *n*-butane, *n*-pentane, *n*-hexane and *n*-octane. First, it is seen that the data are more scattered than those for $\phi = 1.0$ and $\phi = 1.4$, resulting much higher random uncertainty, which makes it difficult to extract a clear trend from them. To observe the trend of the mean flame speeds, Fig. 7(b) plots linear fit of normalized $d\langle R\rangle/dt$ against $Re_{T,f}^{1/2}$ for each fuel at $\phi = 0.8$. The fitted results represent the mean value of experimental data. It is seen that on average the turbulent flame speeds for *n*-octane are lower than *n*-hexane, which in turn are lower than *n*-pentane and *n*-butane. The trend seems to suggest that the turbulent flame speed decreases with the molecular size, although its

validity is limited due to the increased uncertainty. In addition, from Schlieren images we also found that local extinction for *n*-octane and *n*-hexane occurs in larger regions than *n*-butane and *n*-pentane. Finally, Fig. 7(c) plots the linear fit of normalized $d\langle R\rangle/dt$ against $Re_{T,f}^{1/2}$ for all fuels and ϕ. Again, it is seen that at $\phi = 1.0$ and 1.4, the data for all four *n*-alkanes are almost the same.

4. Conclusion

The present study reported turbulent flame speeds for *n*-butane, *n*-pentane, *n*-hexane and *n*-octane, from 1 atm to 5 atm and for a wide range of turbulence intensities and equivalence ratios, using expanding turbulent flames in a fan-stirred vessel. Results show that for stoichiometric and rich mixtures (near-unity *Le*, or $Le < 1$), the normalized turbulent flame speeds of C_4–C_8 *n*-alkanes are almost the same confirming the existence of flame speed similarity as observed for laminar flames. The similar flame speed also suggests that universally large chain *n*-alkanes break down to smaller species with similar reactivity before entering the reaction zone. The flame speed data for these conditions also shows $Re_{T,f}^{1/2}$ dependence which was suggested by our previous work along with other researchers.

The similarity in flame speeds, however, was not observed for lean mixtures ($Le > 1$). The lean conditions were rather characterized by large regions of local extinction for almost all fuels as observed from the Schlieren images. Local extinctions and possible reignition results in large scatter in flame speed data. However, upon averaging, the data suggest that at lean conditions, the turbulent flame speeds decrease with the molecular weight of the fuel. The distinctively different behavior of turbulent flames at lean and rich mixtures at the same turbulence intensities and pressures strongly suggest inclusion of molecular diffusivity or *Le* in defining the regimes of turbulent flames.

Acknowledgments

This research was supported by the Air Force Office of Scientific Research under the technical monitoring of Dr. Chiping Li.

Appendix A. Supplementary data

Supplementary data associated with this article can be found, in the online version, at http://dx.doi.org/10.1016/j.proci.2014.07.070.

References

[1] T. Lu, C.K. Law, *Prog. Energy Combust. Sci.* 35 (2009) 192.
[2] X. You, F.N. Egolfopoulos, H. Wang, *Proc. Combust. Inst.* 32 (2009) 403.
[3] H. Wang, E. Dames, B. Sirjean, et al., Univ. South. Calif., 2010.
[4] C. Ji, E. Dames, Y.L. Wang, H. Wang, F.N. Egolfopoulos, *Combust. Flame* 157 (2010) 277.
[5] A.P. Kelley, A.J. Smallbone, D.L. Zhu, C.K. Law, *Proc. Combust. Inst.* 33 (2011) 963.
[6] F. Wu, A.P. Kelley, C.K. Law, *Combust. Flame* 159 (2012) 1417.
[7] D.F. Davidson, S.C. Ranganath, K.Y. Lam, et al., *Power* 26 (2010) 280.
[8] H.S. Shen, J. Steinberg, J. Vanderover, et al., *Energy Fuels* 23 (2009) 2482.
[9] S.G. Davis, C.K. Law, *Combust. Sci. Technol.* 140 (1998) 427.
[10] C.K. Westbrook, W.J. Pitz, O. Herbinet, H.J. Curran, E.J. Silke, *Combust. Flame* 156 (2009) 181.
[11] E. Ranzi, A. Frassoldati, S. Granata, T. Faravelli, *Ind. Eng. Chem. Res.* 44 (2005) 5170.
[12] J.H. Chen, *Proc. Combust. Inst.* 33 (2011) 99.
[13] F. Wu, C.K. Law, *Combust. Flame* 160 (2013) 2744.
[14] S. Chaudhuri, F. Wu, D. Zhu, C.K. Law, *Phys. Rev. Lett.* 108 (2012) 044503.
[15] S. Chaudhuri, F. Wu, C.K. Law, *Phys. Rev. E* 88 (2013) 033005.
[16] C.K. Law, *Combustion Physics*, Cambridge University Press, New York, 2006.
[17] S.B. Pope, *Turbulent Flows*, Cambridge University Press, 2000.
[18] D. Bradley, M. Lawes, M.S. Mansour, *Combust. Flame* 158 (2011) 123.
[19] S. Chaudhuri, V. Akkerman, C.K. Law, *Phys. Rev. E* 84 (2011) 026322.
[20] N. Peters, *J. Fluid Mech.* 242 (1992) 611.
[21] D. Bradley, M. Lawes, M.S. Mansour, *Proc. Combust. Inst.* 32 (2009) 1587.
[22] S. Chaudhuri, A. Saha, C.K. Law, *Proc. Combust. Inst.* 35, in press.
[23] A.N. Lipatnikov, J. Chomiak, *Prog. Energy Combust. Sci.* 31 (2005) 1.
[24] F. Wu, W. Liang, Z. Chen, Y. Ju, C.K. Law, *Proc. Combust. Inst.* 35 (2014). http://dx.doi.org/10.1016/j.proci.2014.05.065.